Fiber-Shaped Cu-Ion Diffusive Memristor for Neuromorphic Computing

Jialin Meng, Yue Liu, Yuqing Fang, Zhenhai Li, Jieru Song, Tianyu Wang, Hao Zhu, *Member, IEEE*, Peining Chen, Qingqing Sun, David Wei Zhang, and Lin Chen

***Abstract*— Fiber-shaped memristors have attracted enormous attention as potential wearable electronics. Here, a Cu-ion diffusive memristor with fiber shape was proposed for artificial synapse and neuromorphic computing. The fiber-shaped diffusive memristor exhibits gradual conductance modulation characteristics under consecutive voltage sweeps. Typical synaptic plasticity including EPSC, PPF, PPD, LTP/LTD and learning behaviors were all successfully achieved by the memristor. The active Cu^{2+} of diffusive memristor was similar as Ca^{2+} diffusion in biological synapse, which is the basis of realizing the functions of synaptic plasticity. The fiber-shaped Cu^{2+} diffusive memristor acting as artificial synapse paves the way for next-generation wearable neuromorphic computing system.**

***Index Terms*— Textile electronics, memristor, artificial synapse, neuromorphic computing.**

I. INTRODUCTION

INSPIRED by human brain and biological system, neuromorphic computing has become a new computing paradigm with high efficiency and low power consumption [1], [2], [3], [4], [5], which shows great potential in overcoming the bottleneck of von Neumann architecture [6], [7]. In biological neural network, synapses are the basic units for various neuromorphic computing functions [8], [9], [10], [11], [12], [13]. There are 10^{11} neurons and 10^{15} synapses in human brain, where the ions diffusion plays an important role in neurotransmitters release and transmission of biological information [14], [15]. Hence, in order to get closer to the working mode of human brain, developing an emerging ionic diffusive device with high biological similarity to simulate synapse is an effective way to realize high-efficiency brain-inspired neuromorphic computing.

The increasing demands of wearable artificial intelligent devices proposed huge requirements of excellent flexibility for each functional unit. As the core computing unit, flexible neuromorphic computing electronics have attracted great attentions of researchers [16], [17], [18]. Developing flexible neuromorphic computing electronics could increase the wearable comfort and bending reliability of the entire wearable system. On the other hand, the size of traditional computing devices is gradually approaching the physical limit, and the big data computing require integrating more neuromorphic computing devices on a flexible substrate to achieve large-scale parallel computing, which undoubtedly increases the flexibility requirement for computing devices. Various flexible three-terminal transistor and two-terminal memristor have been reported with typical synaptic functions [19], [20], [21], [22], [23], [24], such as excitatory post-synaptic current (EPSC), paired-pulse facilitation (PPF), paired-pulse depression (PPD), long-term potentiation/ depression (LTP/LTD) and so on [25], [26], [27], [28], [29], and [30]. Among different artificial synaptic devices, fiber-shaped memristor is a promising candidate for next-generation flexible neuromorphic hardware [31], which exhibits advantages of natural two-terminal woven structure, high-density integration capability, analogue conductance update and excellent wearability.

In this work, a fiber-shaped Cu-ion (Cu^{2+}) diffusive memristor Cu/CuO/Pt was proposed to simulate bio-synapse for neuromorphic computing. The conductance of device could be modulated by consecutive voltage sweeps, which is based on the movement of Cu^{2+}, similar as biological ion (Ca^{2+}) diffusion. Under increased amplitude of applied spike, the conductance of memristor could be induced to multi-level

---

Manuscript received 12 April 2023; accepted 1 May 2023. Date of publication 10 May 2023; date of current version 28 June 2023. This work was supported in part by the National Key Research and Development Program of China under Grant 2021YFA1202600; in part by NSFC under Grant 92064009 and Grant 22175042; in part by the Science and Technology Commission of Shanghai Municipality under Grant 22501100900; in part by the Shanghai Sailing Program under Grant 23YF1402200 and Grant 23YF1402400; in part by the China Postdoctoral Science Foundation under Grant 2022TQ0068, Grant BX2021070, and Grant 2021M700026; and in part by the Zhejiang Lab's International Talent Fund for Young Professionals. The review of this letter was arranged by Editor S. Yu. *(Jialin Meng and Yue Liu contributed equally to this work.) (Corresponding authors: Tianyu Wang; Peining Chen; Lin Chen.)*

Jialin Meng, Yuqing Fang, Zhenhai Li, Jieru Song, Tianyu Wang, Hao Zhu, Qingqing Sun, David Wei Zhang, and Lin Chen are with the School of Microelectronics, Fudan University, Shanghai 200433, China, also with the Zhangjiang Fudan International Innovation Center, Shanghai 201203, China, and also with the Jiashan Fudan Institute, Jiaxing, Zhejiang 314100, China (e-mail: tywang@fudan.edu.cn; linchen@fudan.edu.cn).

Yue Liu and Peining Chen are with the School of Microelectronics, Fudan University, Shanghai 200433, China, and also with the State Key Laboratory of Molecular Engineering of Polymers, Department of Macromolecular Science, Laboratory of Advanced Materials, Fudan University, Shanghai 200438, China (e-mail: peiningc@fudan.edu.cn).

Color versions of one or more figures in this letter are available at https://doi.org/10.1109/LED.2023.3274828.

Digital Object Identifier 10.1109/LED.2023.3274828

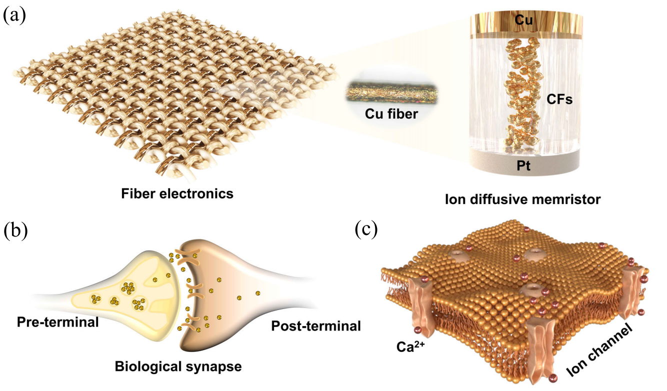

Fig. 1. (a) An illustration of fiber electronics with structure of Cu/CuO/Pt. Inset is the optical image of Cu fiber with CuO film. (b) Schematic diagram of biological synapse, where the neurotransmitters release occurred. (c) The ion diffusion dynamics of biological liquid bilayer membrane, where Ca^{2+} flow through ion channel.

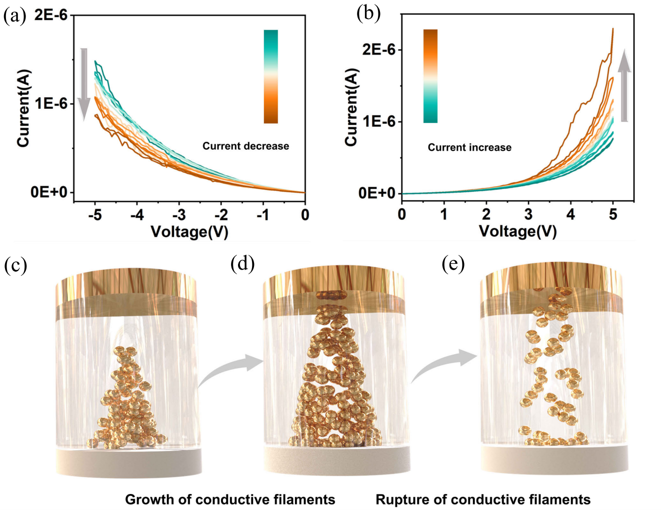

Fig. 2. (a) Consecutive decreased current of memristor under negative voltage sweeping. (b) Consecutive increased current of memristor under positive voltage sweeping. (c) The growth of conductive filaments under positive voltage. (d) The state of device under low resistance state. (e) Rupture of conductive filaments under negative voltage.

states. Furthermore, the synaptic memristor exhibits typical synaptic plasticity, including EPSC, PPF, PPD, LTP/LTD and learning behaviors. The conductance states of fiber-shaped memristor array are stable before and after bending operations, which paves the way for application of the device in wearable neuromorphic computing system.

II. EXPERIMENTAL DETAILS

Firstly, the Cu fibers (Alfa Aesar) and Pt fibers (Alfa Aesar) were used as top electrode and bottom electrode, which were cleaned with acetone, ethanol and deionized water for 5 min. Then, the active layer of CuO was in-situ grown on the Cu fibers via an anodic oxidation method, where the Cu fiber act as anode and the time was controlled at 10 min in the fabrication process. After deposition process, the structure of Cu/CuO fibers were obtained. Lastly, the Pt fibers were interwoven with Cu/CuO fibers to form fiber-shaped memristors. Electrical measurement was carried out by semiconductor parameter analyzer (Agilent B1500).

III. RESULTS AND DISCUSSION

Textile electronics with interwoven structure are emerging wearable devices, showing great potential in flexibility and portability. As shown in Fig. 1a, Cu fiber with CuO film acts as the core unit of fiber-shaped ion diffusive memristor. The top of Cu fiber and bottom electrodes of Pt fiber act as pre-terminal and post-terminal of bio-synapse in Fig. 1b, respectively. In the active layer of CuO film, Cu^{2+} diffusion could lead to conductance modulation of memristor, similar as weight update process in biological synapse. Fig. 1c shows the detailed ion diffusion process in liquid bilayer membrane, where the biological ions of Ca^{2+} could flow through ion channel and induce the change of membrane potential. The natural similarity of ion diffusion process in the fiber-shaped memristor and biology lays the foundation for the simulation of synaptic plasticity by artificial synaptic device.

The conductance of fiber-shaped Cu^{2+} diffusive memristor show excellent analog switching characteristics under different voltages, which was due to the growth and rupture of conductive filaments (CFs) [32]. As shown in Fig. 2a, the current values gradually decreased under consecutive negative voltage sweeping from 0 V to −5 V, indicating the inhibition capability of synaptic weights in the simulation of bio-synapse. Fig. 2b shows enhanced current of memristor under consecutive positive voltage sweeping from 0 V to 5 V, indicating the potential of device in simulating synaptic weight update. In order to better understand the physical mechanism of ion diffusive memristor, we plot the schematic diagram of conductive filaments in active layer. Fig. 2c-Fig. 2d show the growth process of CFs in active layer, where the Cu^{2+} diffused to the bottom electrode and turned to Cu atoms. CFs were gradually formed with the accumulation of Cu atoms. The CFs gradually broke when opposite voltage was applied. Fig. 2d-Fig. 2e show the rupture process of CFs, resulting in the decrease of device conductance.

Biological synapse could transfer information between pre-terminal neuron and post-terminal neuron by the release of neurotransmitters, which ensures the realization of various biological synaptic functions and complex neuromorphic computing. The first step of achieving neuromorphic computing is to simulate synaptic plasticity based on artificial synaptic device [1]. In this work, typical synaptic plasticity was successfully emulated by the Cu-ion diffusive memristor. As shown in Fig. 3a, excitatory synaptic behavior was trigged by different voltage amplitude. As the increase of pulse amplitude from 1.2 V, 1.5 V, 2 V, 2.5 V to 3V, the post-synaptic current increased from 146 nA, 151 nA, 166 nA, 188 nA and 205 nA, respectively. The result demonstrates that the memristor could achieve spike-amplitude dependent plasticity (SADP) as biological synapse.

The synaptic behaviors of PPF and PPD are considered to be important to the functions of decoding temporal visual information in biology [7]. PPF and PPD could be mimicked when a pair of pre-synaptic spikes were applied to pre-terminal of memristor, as shown in Fig. 3b. The consecutive two

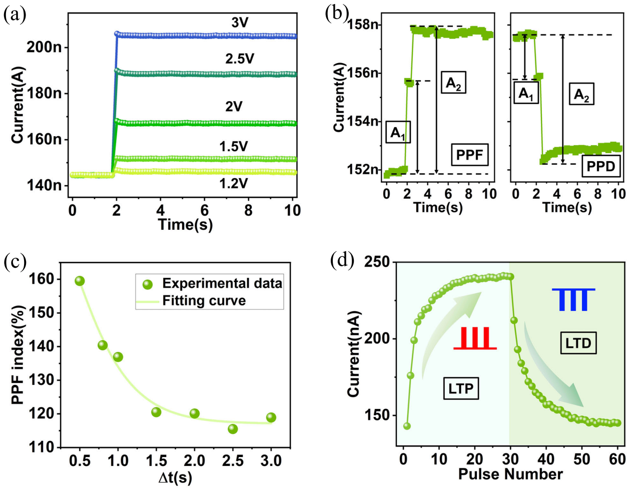

Fig. 3. (a) EPSC of memristor under different voltage amplitudes (1.2 V, 1.5 V, 2 V, 2.5 V and 3 V). (b) PPF and PPD characteristics of artificial synaptic device. (c) PPF index of device with different time interval. (d) LTP/LTD behaviors of memristor under 30 positive pulses and 30 negative pulses.

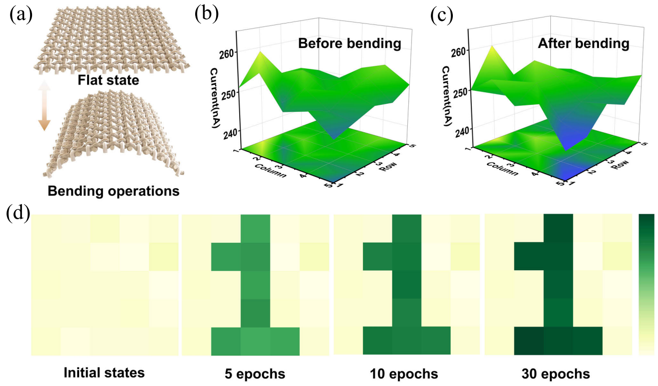

Fig. 4. (a) Schematic diagram of bending fiber-shaped memristor. (b) Current mapping images of 5 × 5 fiber-shaped memristor array before bending operation. (c) Current mapping images of device array after 100 cycles bending operation. (d) Array learning of number “1” based on 5 × 5 memristor array under initial state, 5 epochs, 10 epochs and 30 epochs.

positive pulses (1.5 V, 10 ms) with interval of 500 ms could induced two enhanced post-synaptic current, where the first current spike (A_1) is lower than the second current spike (A_2). Furthermore, PPF index ($A_2/A_1 \times 100\%$) was calculated and shown in Fig. 3c. Instead, when two negative pulses (−1.5 V, 10 ms) with interval of 500 ms applied to device, two inhibitory current spikes were induced. Long-term plasticity including LTP/LTD are critical to the functions of learning, memory and neuromorphic computing in human brain. Fig. 3d shows the LTP/LTD behavior emulated by memristor, which was induced by consecutive 30 pulses (2 V, 10 ms for LTP and −2 V, 10 ms for LTD). The consecutive conductance modulation characteristic paves the way for memristor achieving weights update as bio-synapse.

A fiber-shaped memristor array of 5 × 5 was proposed to investigate the flexibility and learning functions of artificial synapses. Fig. 4a shows schematic of textile memristor under flat state and bending operations. The 5 × 5 current mapping of largest values in LTP (245 nA∼ 259 nA) were statistically plotted in Fig. 4b. After 100 cycles bending operations (bending radius of 10 mm), the stable current mapping (242 nA∼ 260 nA) reveals excellent reliability of fiber-shaped memristor, as shown in Fig. 4c. Furthermore, array level learning functions were verified in Fig. 4d. The digit of “1” could be learned by the 5 × 5 memristor array with increased pulse number (0, 5, 10, 30 epochs). The contour of digit “1” was gradually clear under increased pulse number from 0 to 30 epochs, indicating that the learning effect is gradually deepened. This enhanced conductance process of digit is analogous to the repeated learning of information to enhance memory effect in human brain.

IV. CONCLUSION

In summary, the fiber-shaped Cu^{2+} diffusive memristor has been proposed for neuromorphic computing, where the Cu^{2+} migration is similar to the biological ion diffusion process. Under different voltage stimulation, the artificial synaptic memristor could emulate typical synaptic functions, including EPSC, SADP, PPF, PPD and LTP/LTD. By constructing a 5 × 5 memristor array, the array level learning behaviors of digit “1” was verified. These results indicate that the fiber-shaped memristor have potentials in next-generation wearable neuromorphic computing system.

REFERENCES

[1] J. Meng, T. Wang, H. Zhu, L. Ji, W. Bao, P. Zhou, L. Chen, Q.-Q. Sun, and D. W. Zhang, “Integrated in-sensor computing optoelectronic device for environment-adaptable artificial retina perception application,” *Nano Lett.*, vol. 22, no. 1, pp. 81–89, Jan. 2022, doi: 10.1021/acs.nanolett.1c03240.

[2] G. Li, D. Xie, H. Zhong, Z. Zhang, X. Fu, Q. Zhou, Q. Li, H. Ni, J. Wang, E.-J. Guo, M. He, C. Wang, G. Yang, K. Jin, and C. Ge, “Photo-induced non-volatile VO_2 phase transition for neuromorphic ultraviolet sensors,” *Nature Commun.*, vol. 13, no. 1, p. 1729, Apr. 2022, doi: 10.1038/s41467-022-29456-5.

[3] H. H. Chouhdry, D. H. Lee, A. Bag, and N.-E. Lee, “A flexible artificial chemosensory neuronal synapse based on chemoreceptive ionogel-gated electrochemical transistor,” *Nature Commun.*, vol. 14, no. 1, p. 821, Feb. 2023, doi: 10.1038/s41467-023-36480-6.

[4] J. Guo, L. Liu, B. Bian, J. Wang, X. Zhao, Y. Zhang, and Y. Yan, “Field-created coordinate cation bridges enable conductance modulation and artificial synapse within metal nanoparticles,” *Nano Lett.*, vol. 22, no. 16, pp. 6794–6801, Aug. 2022, doi: 10.1021/acs.nanolett.2c02675.

[5] J. Qiu, J. Cao, X. Liu, P. Chen, G. Feng, X. Zhang, M. Wang, and Q. Liu, “A flexible organic electrochemical synaptic transistor with dopamine-mediated plasticity,” *IEEE Electron Device Lett.*, vol. 44, no. 1, pp. 176–179, Jan. 2023, doi: 10.1109/LED.2022.3225143.

[6] K. Liang, H. Ren, Y. Wang, D. Li, Y. Tang, C. Song, Y. Chen, F. Li, H. Wang, and B. Zhu, “Tunable plasticity in printed optoelectronic synaptic transistors by contact engineering,” *IEEE Electron Device Lett.*, vol. 43, no. 6, pp. 882–885, Jun. 2022, doi: 10.1109/LED.2022.3166507.

[7] T. Wang, J. Meng, Z. He, L. Chen, H. Zhu, Q. Sun, S. Ding, P. Zhou, and D. W. Zhang, “Ultralow power wearable heterosynapse with photoelectric synergistic modulation,” *Adv. Sci.*, vol. 7, no. 8, Apr. 2020, Art. no. 1903480, doi: 10.1002/advs.201903480.

[8] K. Liang, R. Wang, B. Huo, H. Ren, D. Li, Y. Wang, Y. Tang, Y. Chen, C. Song, F. Li, B. Ji, H. Wang, and B. Zhu, “Fully printed optoelectronic synaptic transistors based on quantum dot-metal oxide semiconductor heterojunctions,” *ACS Nano*, vol. 16, no. 6, pp. 8651–8661, Jun. 2022, doi: 10.1021/acsnano.2c00439.

[9] S. G. Sarwat, B. Kersting, T. Moraitis, V. P. Jonnalagadda, and A. Sebastian, “Phase-change memtransistive synapses for mixed-plasticity neural computations,” *Nature Nanotechnol.*, vol. 17, no. 5, pp. 507–513, May 2022, doi: 10.1038/s41565-022-01095-3.

[10] J.-L. Meng, T.-Y. Wang, L. Chen, Q.-Q. Sun, H. Zhu, L. Ji, S.-J. Ding, W.-Z. Bao, P. Zhou, and D. W. Zhang, "Energy-efficient flexible photoelectric device with 2D/0D hybrid structure for bio-inspired artificial heterosynapse application," *Nano Energy*, vol. 83, May 2021, Art. no. 105815, doi: 10.1016/j.nanoen.2021.105815.

[11] D. Kumar, A. Saleem, L. B. Keong, A. Singh, Y. H. Wang, and T. Tseng, "$ZnSnO_y$/$ZnSnO_x$ bilayer transparent memristive synaptic device for neuromorphic computing," *IEEE Electron Device Lett.*, vol. 43, no. 8, pp. 1211–1214, Aug. 2022, doi: 10.1109/LED.2022.3186055.

[12] Z. Hua, B. Yang, J. Zhang, D. Hao, P. Guo, J. Liu, L. Jiang, and J. Huang, "Monolayer molecular crystals for low-energy consumption optical synaptic transistors," *Nano Res.*, vol. 15, no. 8, pp. 7639–7645, Aug. 2022, doi: 10.1007/s12274-022-4372-9.

[13] Z. Lv, Y. Zhou, S.-T. Han, and V. A. L. Roy, "From biomaterial-based data storage to bio-inspired artificial synapse," *Mater. Today*, vol. 21, no. 5, pp. 537–552, Jun. 2018, doi: 10.1016/j.mattod.2017.12.001.

[14] J. Meng, Z. Li, Y. Fang, Q. Li, Z. He, T. Wang, H. Zhu, L. Ji, Q. Sun, D. W. Zhang, and L. Chen, "Li-ion doped artificial synaptic memristor for highly linear neuromorphic computing," *IEEE Electron Device Lett.*, vol. 43, no. 12, pp. 2069–2072, Dec. 2022, doi: 10.1109/LED.2022.3211520.

[15] X. Zhu, D. Li, X. Liang, and W. D. Lu, "Ionic modulation and ionic coupling effects in MoS_2 devices for neuromorphic computing," *Nature Mater.*, vol. 18, no. 2, pp. 141–148, Feb. 2019, doi: 10.1038/s41563-018-0248-5.

[16] T.-Y. Wang, J.-L. Meng, M.-Y. Rao, Z.-Y. He, L. Chen, H. Zhu, Q.-Q. Sun, S.-J. Ding, W.-Z. Bao, P. Zhou, and D. W. Zhang, "Three-dimensional nanoscale flexible memristor networks with ultralow power for information transmission and processing application," *Nano Lett.*, vol. 20, no. 6, pp. 4111–4120, Jun. 2020, doi: 10.1021/acs.nanolett.9b05271.

[17] W. S. Wang, Z. Y. Ren, Z. W. Shi, H. Xiao, Y. H. Zeng, and L. Q. Zhu, "Flexible nanocellulose gated pseudo-diode for neuromorphic electronic applications," *IEEE Electron Device Lett.*, vol. 43, no. 5, pp. 737–740, May 2022, doi: 10.1109/LED.2022.3160494.

[18] Y. Lee, J. Y. Oh, W. Xu, O. Kim, T. R. Kim, J. Kang, Y. Kim, D. Son, J. B.-H. Tok, M. J. Park, Z. Bao, and T.-W. Lee, "Stretchable organic optoelectronic sensorimotor synapse," *Sci. Adv.*, vol. 4, no. 11, Nov. 2018, Art. no. eaat7387, doi: 10.1126/sciadv.aat7387.

[19] Y. Zhang, L. Liu, B. Tu, B. Cui, J. Guo, X. Zhao, J. Wang, and Y. Yan, "An artificial synapse based on molecular junctions," *Nature Commun.*, vol. 14, no. 1, p. 247, Jan. 2023, doi: 10.1038/s41467-023-35817-5.

[20] J.-L. Meng, T.-Y. Wang, Z.-Y. He, L. Chen, H. Zhu, L. Ji, Q.-Q. Sun, S.-J. Ding, W.-Z. Bao, P. Zhou, and D. W. Zhang, "Flexible boron nitride-based memristor for *in situ* digital and analogue neuromorphic computing applications," *Mater. Horizons*, vol. 8, no. 2, pp. 538–546, 2021, doi: 10.1039/D0MH01730B.

[21] X. Wu, S. Wang, W. Huang, Y. Dong, Z. Wang, and W. Huang, "Wearable in-sensor reservoir computing using optoelectronic polymers with through-space charge-transport characteristics for multi-task learning," *Nature Commun.*, vol. 14, no. 1, p. 468, Jan. 2023, doi: 10.1038/s41467-023-36205-9.

[22] K. J. Kwak, J. H. Baek, D. E. Lee, I. H. Im, J. Kim, S. J. Kim, Y. J. Lee, J. Y. Kim, and H. W. Jang, "Ambient stable all inorganic $CsCu_2I_3$ artificial synapses for neurocomputing," *Nano Lett.*, vol. 22, no. 14, pp. 6010–6017, Jul. 2022, doi: 10.1021/acs.nanolett.2c01272.

[23] J. Meng, T. Wang, Z. He, Q. Li, H. Zhu, L. Ji, L. Chen, Q. Sun, and D. W. Zhang, "A high-speed 2D optoelectronic in-memory computing device with 6-bit storage and pattern recognition capabilities," *Nano Res.*, vol. 15, no. 3, pp. 2472–2478, Mar. 2022, doi: 10.1007/s12274-021-3729-9.

[24] S. Zhang, J. Guo, L. Liu, H. Ruan, C. Kong, X. Yuan, B. Zhang, G. Gu, P. Cui, G. Cheng, and Z. Du, "The self-powered artificial synapse mechanotactile sensing system by integrating triboelectric plasma and gas-ionic-gated graphene transistor," *Nano Energy*, vol. 91, Jan. 2022, Art. no. 106660, doi: 10.1016/j.nanoen.2021.106660.

[25] Z. Zhao, A. Abdelsamie, R. Guo, S. Shi, J. Zhao, W. Lin, K. Sun, J. Wang, J. Wang, X. Yan, and J. Chen, "Flexible artificial synapse based on single-crystalline $BiFeO_3$ thin film," *Nano Res.*, vol. 15, no. 3, pp. 2682–2688, Mar. 2022, doi: 10.1007/s12274-021-3782-4.

[26] T. Guo, J. Ge, B. Sun, K. Pan, Z. Pan, L. Wei, Y. Yan, Y. N. Zhou, and Y. A. Wu, "Soft biomaterials based flexible artificial synapse for neuromorphic computing," *Adv. Electron. Mater.*, vol. 8, no. 10, Oct. 2022, Art. no. 2200449, doi: 10.1002/aelm.202200449.

[27] R. Ji, G. Feng, C. Jiang, B. Tian, C. Luo, H. Lin, X. Tang, H. Peng, and C. Duan, "Fully light-modulated organic artificial synapse with the assistance of ferroelectric polarization," *Adv. Electron. Mater.*, vol. 8, no. 7, Jul. 2022, Art. no. 2101402, doi: 10.1002/aelm.202101402.

[28] G. Zhou, Z. Wang, B. Sun, F. Zhou, L. Sun, H. Zhao, X. Hu, X. Peng, J. Yan, H. Wang, W. Wang, J. Li, B. Yan, D. Kuang, Y. Wang, L. Wang, and S. Duan, "Volatile and nonvolatile memristive devices for neuromorphic computing," *Adv. Electron. Mater.*, vol. 8, no. 7, Jul. 2022, Art. no. 2101127, doi: 10.1002/aelm.202101127.

[29] Y. Fang, J. Meng, Q. Li, T. Wang, H. Zhu, L. Ji, Q. Sun, D. W. Zhang, and L. Chen, "Two-terminal photoelectric dual modulation synaptic devices for face recognition," *IEEE Electron Device Lett.*, vol. 44, no. 2, pp. 241–244, Feb. 2023, doi: 10.1109/LED.2022.3228944.

[30] X. Chen, E. Li, X. Zhang, Q. Chen, R. Yu, Y. Ye, H. Chen, and T. Guo, "Printed organic synaptic transistor array for one-to-many neural response," *IEEE Electron Device Lett.*, vol. 43, no. 3, pp. 394–397, Mar. 2022, doi: 10.1109/LED.2022.3144662.

[31] T. Wang, J. Meng, X. Zhou, Y. Liu, Z. He, Q. Han, Q. Li, J. Yu, Z. Li, Y. Liu, H. Zhu, Q. Sun, D. W. Zhang, P. Chen, H. Peng, and L. Chen, "Reconfigurable neuromorphic memristor network for ultralow-power smart textile electronics," *Nature Commun.*, vol. 13, no. 1, p. 7432, Dec. 2022, doi: 10.1038/s41467-022-35160-1.

[32] B. C. Jang, S. Kim, S. Y. Yang, J. Park, J.-H. Cha, J. Oh, J. Choi, S. G. Im, V. P. Dravid, and S.-Y. Choi, "Polymer analog memristive synapse with atomic-scale conductive filament for flexible neuromorphic computing system," *Nano Lett.*, vol. 19, no. 2, pp. 839–849, Feb. 2019, doi: 10.1021/acs.nanolett.8b04023.